Modulation of Akt-p38-MAPK/Nrf2/SIRT1 and NF-κB pathways by Wine Pomace Product in hyperglycemic endothelial cell line.

Gisela Gerardi, Mónica Cavia-Saiz*, María D. Rivero-Pérez, María L. González-SanJosé and Pilar Muñiz

Department of Biotechnology and Food Science, Faculty of Sciences, University of Burgos, Plaza Misael Bañuelos, 09001, Burgos, Spain.

***Corresponding author**: Dra. Mónica Cavia Saiz, Plaza Misael Bañuelos, Facultad de Ciencias, Departamento de Biotecnología y Ciencia de los Alimentos, 09001, Burgos, Spain.

E-mail: monicacs@ubu.es

Phone: +34-947258800 Ext. 8210

Fax: +34-947258831

Email addresses: Gisela Gerardi (mggerardi@ubu.es), Monica Cavia-Saiz (monicacs@ubu.es), María D. Rivero-Pérez (drivero@ubu.es), María L. González-SanJosé (marglez@ubu.es), Pilar Muñiz (pmuniz@ubu.es).

Abstract

Wine by-products show great potential as source of bioactive compounds that protect the vascular endothelial function by the modulation of both Nrf2 and Nf-κB pathways. This study investigates the pathways involved in the effects of a red wine pomace product (rWPP) against inflammatory and oxidative damage in hyperglycemic EA.hy926 endothelial cells. rWPP-digested fractions showed an inhibitory effect on IKK/IκBα/NF-κB pathway and a stimulatory effect on Akt-p38-MAPK/Nrf2 pathway with an impact on their antioxidant and anti-inflammatory downstream targets. In addition, the pathways regulation was also accompanied by downregulation of the gene expression of superoxide dismutase 2, cyclooxygenase 2 and NADPH oxidase 4. These results suggest the expression of SOD2 as an early adaptive response to the inflammatory effect mediated by NF-κB in hyperglycemic cells, and the treatment with the rWPP-digested fractions regulate this inflammatory process by Nrf2 pathway increased expression of antioxidant enzymes.

Keywords:

Polyphenols, wine pomace, endothelial dysfunction, NF-κB, Nrf2, p38 MAPK, Akt, SIRT1, oxidative stress, EA.hy926, phase 2 enzymes, SOD2, NOX4, COX2.

Abbreviations:

Akt, protein kinase B; **AREs**, antioxidant responsive elements; **CAT**, catalase; **COX2,** ciclooxigenase 2; **eNOS**, endothelial nitric oxide synthase; **GAPDH**, glyceraldehyde-3-phosphate dehydrogenase; **GCLC**, glutamate-cysteine ligase catalytic subunit; **GPX1**, glutathione peroxidase 1; **GR,** glutathione reductase; **GS,** glutathione syntase; **GSH,** glutathione; **GSSG,** glutathione disulfide; **HO1**, hemo oxygenase 1; **IκBα,** inhibitor of kappa B; **IKK,** IκB kinase; **NF-κB**, nuclear factor-kappa B; **NO,** nitric oxide; **NOX4**, NADPH oxidase 4; **NQO1**, NAD(P)H:quinone oxidoreductase 1; **Nrf2**, nuclear factor erythroid 2-related factor 2; **p38-MAPK**, p38 mitogen-activated protein kinase; **PI3K,** phosphatidylinositol 3-kinase; **ROS**, reactive oxygen species; **rWPP**, red wine pomace product; **SIRT1,** sirtuin 1; **SOD1**, superoxide dismutase 1; **SOD2**, superoxide dismutase 2; **WPGI**, wine pomace potentially bioavailable fraction obtained after simulated gastrointestinal digestion; **WPF**, wine pomace potentially bioavailable fraction obtained after simulated colonic fermentation.

1 Introduction

Endothelial dysfunction plays a critical role in the pathogenesis and development of vascular diseases, involving a close relation between oxidative stress, inflammatory process and an altered vascular endothelial function. Hyperglycemia, with elevated pro-inflammatory mediators and oxidative stress, is common to many vascular diseases and is consistent with high nuclear factor-kappa B (NF-κB) activity and impaired nuclear factor erythroid 2-related factor 2 (Nrf2) activity (Battino et al., 2018; Gopalakrishnan & Tony Kong, 2008). There is therefore abundant evidence for inverse regulation of Nrf2 and NF-κB in vascular disease. For instance, the role of Nrf2 in reducing inflammation has been linked to its ability of antagonize NF-κB (Pedruzzi, Stockler-Pinto, Leite, & Mafra, 2012).

Recent studies have suggested that the polyphenols of a red Wine Pomace Product (rWPP) (García-Lomillo, González-SanJosé, Del Pino-García, Rivero-Pérez, & Muñiz-Rodríguez, 2014) could have a capacity to modulate endothelial dysfunction through increased levels of NO and decreased levels of ROS (Del Pino-García, Gerardi, Rivero-Pérez, González-SanJosé, et al., 2016; Del Pino-García, Rivero-Pérez, González-SanJosé, Croft, & Muñiz, 2017). The efficacy of rWPP may be due to its highly biologically active compounds but the molecular mechanisms of this potentially beneficial product have yet to be clearly elucidated.

Some polyphenols have an effect on the IKK/IκBα/NF-κB pathway (Afrin et al., 2018). For instance, IKK contains thiol groups that are sensitive to metabolites of flavonols (Son et al., 2010). Furthermore, polyphenols act in many varied co-regulation mechanisms between NF-κB and Nrf2 by the regulation of Sirtuin 1 (SIRT1) activity (Chung et al., 2010; K. Huang, Gao, & Wei, 2017; Lakshminarasimhan, Rauh, Schutkowski, & Steegborn, 2013; Yeung et al., 2004) and by affecting phosphorylation that is mediated by kinases such as MAPK, PI3K/Akt and PKC (Eggler, 2013; H. Huang, Nguyen, & Pickett, 2002).

Based on the above data, it is important to confirm whether Nrf2 activation by polyphenols is due either to NF-κB inhibition, or to other independent mechanisms. Hence, the aim of the present study was to elucidate the possible pathways involved in the potentially protective effects of rWPP from a winery against endothelial dysfunction under hyperglycemic conditions. In accordance with that objective, Akt-p38-MAPK/Nrf2 and IKK/IκBα/NF-κB pathways and the possible adaptive response of the enzyme SOD2 in the EA.Hy926 endothelial cell line were analyzed under hyperglycemic conditions, to establish possible action mechanisms of phenolic compounds. Considering previous studies in which changes in the structure and activity of polyphenols were observed after digestion of rWPP (Del Pino-García, Gerardi, Rivero-Pérez,

González-SanJosé, et al., 2016; Del Pino-García, González-Sanjosé, Rivero-Pérez, García-Lomillo, & Muñiz, 2016; Del Pino-García, Rivero-Pérez, González-SanJosé, Croft, & Muñiz, 2016), an in vitro gastrointestinal digestion and colonic fermentation were performed.

2 Materials and methods

2.1 Red wine pomace product

Red wine pomace-derived product from the vinification of *Vitis vinífera L. cv. Tempranillo* was prepared at the University of Burgos. This product was obtained from seedless red wine pomace using a heat treatment as stabilization process, and its main characteristics and composition was determined (Table S1 and S2, Supplementary Material).

2.2 *In vitro* gastrointestinal digestion and colonic fermentation of the rWPP

The *in vitro* digestion of the red wine pomace product (rWPP) was performed as previously described (Del Pino-García, Gerardi, Rivero-Pérez, González-SanJosé, et al., 2016; Del Pino-García, Rivero-Pérez, González-SanJosé, et al., 2016). This procedure mainly involved two sequential phases that simulate conditions along the gut: enzymatic gastrointestinal digestion and colonic fermentation. A dialysis step was performed to model the passive absorption of the intestinal barrier and obtain potentially bioavailable fractions. The two fractions obtained was labelled as 'WPGI' (Wine Pomace potentially bioavailable fraction after GastroIntestinal digestion) and 'WPF' (Wine Pomace potentially bioavailable fraction after colonic Fermentation). Three replicates were carried out for each fraction. Negative digested controls (without rWPP) for both types of fractions were also prepared.

2.3 Quantification of phenolic compounds

Concentration of phenolic acids were measured using a gas chromatography coupled to electron ionization mass spectrometry (GC-EI-MS) method previously described (Del Pino-García, Rivero-Pérez, González-SanJosé, et al., 2016), with some modifications. Samples (1mg of dried fraction) were directly derivatized with 50 μL of BSTFA and 50 μL of dry pyridine, mixed and heated at 40 °C for 30 min. The trimethylsilyl (TMS) derivatives obtained were analyzed on an Agilent 7890B GC System (Agilent Technologies, Inc., Palo Alto, CA) coupled to an Agilent 7010 GC/MS TripleQuad detector and fitted with an DB5- MS column (25 m x 0.20 mm, 0.33 μm film thickness, Agilent Technologies) using helium as the carrier gas. For quantification, calibration curves were established by measuring peak areas versus response in comparison

with the internal standard 1-Hydroxy-2-naphthoic acid over a range of each analyte concentrations. The concentration of phenolic acids was finally expressed as μg/g digested fraction.

The identification and quantification of stilbenes, flavan-3-ols and flavonols present on the digested fractions were performed as previously described (Del Pino-García et al., 2017; Pérez-Magariño, Ortega-Heras, & Cano-Mozo, 2008). Briefly, the determinations were carried out using analytical reversed-phase HPLC on an Agilent 1100 series HPLC system (Agilent Technologies Inc., Palo Alto, CA, USA) coupled to a diode array detector. A Spherisorb3® ODS2 reversed phase C18 column (250 mm x 4.6 mm, 3 μm particle size; Waters S.A., Barcelona, Spain) was used. The chromatographic conditions were as follows: flow, 0.6 mL/min; injection volume, 200 μL; mobile phases: A, water:glacial acetic acid (98:2, v/v); B, water:acetonitrile:glacial acetic acid (78:20:2, v/v/v); C, acetonitrile. The solvent gradient used was: 0-25 min, linear gradient from 0-100% to 25-75% of B in A; 25-60 min, linear gradient from 25-75% to 70-30% of B in A; 60-100 min, linear gradient from 70-30% to 100-0% of B in A; 100-120 min, 100% B; 120-130 min; linear gradient from 0-100% to 100-0% of C in B; 130-140 min, 100% C; 140-150 min; linear gradient from 100-0% to 0-100% of C in A. The eluent was monitored at 254, 280, 320, 360, and 520 nm, with compound spectra being obtained between 220 and 600 nm. Peak identification was performed by comparison of retention times and diode array spectral characteristics with the standards. The results were expressed in μg/g digested fraction.

2.4 Cell culture and treatment

The immortalized endothelial cell line EA.hy926 was kindly provided by Dr. Diana Hernández-Romero (IMIB-Arrixaca/UM, Murcia, Spain) and cultured at 37ºC and 5% CO2 in Dulbecco's Eagle's medium (DMEN) 5.6 mM D-glucose or medium high in glucose, 25 mM D-glucose, supplemented with 10% fetal bovine serum (FBS), 2mM L-glutamine and 1% penicillin/streptomycin. Cells were grown in complete culture medium for 24 h and then were exposed for 24 h to 2.5 μg GAE/mL of the WPGI or the WPF. The concentration of the digested fractions used during cell treatment is based in previous bioavailability studies (Del Pino-García, Gerardi, Rivero-Pérez, González-SanJosé, et al., 2016; Scalbert & Williamson, 2000) showing no significant toxicity to cells and optimal efficacy in specific biochemical assays. Normoglycemic cells were only incubated with DMEM 5.6 mM and hyperglycemic cells with the medium high in glucose (25 mM D-glucose).

2.5 Cell viability assessment

Cell viability was analysed using the MTT method (Twentyman & Luscombe, 1987). The results were expressed as % cell viability with respect to normoglycemic control cells.

2.6 Quantitative real-time PCR (qPCR) analysis

Total RNA was isolated from cell suspensions using TRI Reagent solution (Applied Biosystems, Foster City, CA, USA). After treatment with DNase I (Thermo Fisher Scientific, Inc., Waltham, MA, USA), 1 μg of total RNA was reverse-transcribed using a First Strand cDNA Synthesis kit (Thermo Fisher Scientific), and finally amplified using iQ™ SYBR®Green Supermix (Bio-Rad Laboratories, S.A., Madrid, Spain). All the procedures were performed according to the manufacturers' protocols. The sequences of primer sets (forward and reverse) used are listed in the Table 3 of Supplementary Material. qPCR was carried out with an iCycler iQ Real-Time PCR Detection System (Bio-Rad Laboratories, S.A., Madrid, Spain) under the following conditions: 1 cycle at 95 ºC for 3 min, followed by 45 cycles at 95 ºC for 15 s and 60 ºC for 30 s. Data for comparative analysis of gene expression were obtained using the 2(-Delta Delta C(T)) method. Relative gene expression was finally expressed as folds of change compared to normoglycemic control cells.

2.7 Western blotting analysis

Extraction of total proteins was performed by cells sonication in ice-cold lysis buffer (Cell Lysis Buffer, Cell Signaling Technology, Davers, MA, USA). Protein concentration was measured using a protein assay reagent (Quick Start™ Bradford Protein Assay, Bio-Rad, Hercules, CA, USA). Total protein (40 □g) was treated with Laemmli buffer, boiled for 5 min and resolved by 10% SDS-PAGE (Bio-Rad Mini-Protean Tetra cell). Then, protein were electrophoretically transferred (Bio-Rad Trans-Blot Turbo Blotting System) into a PVDF membranes (Bio-Rad Laboratories, Hercules, CA, USA) and incubated overnight at 4ºC with specific primary rabbit antibodies (1:1000) against p38-MAPK, phospho-p38-MAPK, Akt, pAkt, Nrf2, pNrf2, NF-κB p65, pNF-κB p65, IKKαβ, pIKKαβ, IκBα, pIκBα (Cell Signaling Technology, MA, USA), and actin (Sigma-Aldrich). After rinsing, the membranes were incubated with a horseradish-peroxidase-labelled secondary antibody antirrabit (1:3000, Anti-rabbit IgG-HRP-linked Antibody, Cell Signalling Technology, Danvers, MA, USA). Inmunodetection was performed using enhanced chemiluminiscence kit (Clarity Western ECL substrate, Biorad Laboratories, Hercules, CA, USA) and developed using autoradiography (Amersham Hyperfilm ECL, GE Heaalthcare). Proteins bands were quantified by densitometry using the ImageJ software and their relative amounts were normalized to the housekeeping

protein β-actin. The results were expressed as a ratio of the phosphorylated target protein amount against the total target protein.

2.8 Glutathione reduced/oxidized (GSH/GSSG) ratio analysis

Cell GSH and GSSG levels were determined using the Cayman's GSH assay kit (Cayman Chemical, Co., Ann Arbor, MI, USA). All these assays followed the manufacturer's instructions. The results were expressed as a GSH/GSSG ratio.

2.9 Data presentation and statistical analysis

The results were expressed as means ± standard deviation of independent experiments (n=3). Statistical analysis was performed using Statgraphics® Centurion XVI, version 16.2.04 (Statpoint Technologies, Inc., Warranton, VA, USA). Shapiro-Wilk test ($p > 0.05$) was used to determine the normal distribution of the samples. Student's t test was used to determine significant differences between WPGI and WPF. One-way analysis of variance (ANOVA), using Fisher's least significant difference (LSD) test, was used to determine significant differences ($p < 0.05$) between data from cells incubated with the different treatments.

3 Results

The results presented in the Table 1 detail a complete chemical study of the polyphenolic composition of the both rWPP-digested fractions, colonic fermentation (WPF) and gastrointestinal fraction (WPGI). These results demonstrated that the fractions obtained from WPF had a high content of non-flavonoid polyphenols, principally hydroxycinnamic acids (89.1 ± 15.8 µg/g rWPP) and resveratrol (1.37 ± 0.13 µg/g) and flavonoids such as the flavan-3-ols epigallocatechin (43.2 ± 2.14 µg/g) and procyanidin B1 (130 ± 12 µg/g). Likewise, the digested fraction WPGI had a high content of flavonols myricetin-3-O-rhamnoside (39.2 ± 1.54 µg/g) and kaempferol-3-O rutinoside (81.6 ± 11 µg/g).

The effects of the treatment with WPGI and WPF fractions on hyperglycemic and normoglycemic cells viability not showed cytotoxicity at the doses evaluated (Figure S1, Supplementary Material).

The figure 1 illustrated the regulatory effect of the hyperglycemia and the rWPP-digested fractions on the Nrf2 mRNA expression and the pNrf2/Nrf2 ratio in cells. The hyperglycemic (HG) conditions in the endothelial cells results in a significant reduction of a 60% in the Nrf2 mRNA levels expression (Figure 1A) and a 40% reduction in the pNrf2/Nrf2 ratio (Figure 1B) in comparison with normoglycemic cells (NG). The treatment of the hyperglycemic cells with WPGI and WPF increased the mRNA levels of Nrf2 (19.0 and

29.0% increased, respectively, in comparison with the HG) and the protein expression of pNrf2/Nrf2 to reach the levels of the NG cells.

The Akt and p38-MAPK regulation by the rWPP-digested fractions was evaluated by western blot expression and the results are showed in Figure 2. The p-Akt/Akt ratio (Figure 2B) increased significantly by 42.3 and 45% in the hyperglycemic cells treated with WPGI and WPF compared to the untreated hyperglycemic cells (HG). However, the phospho-p38-MAPK/p38-MAPK ratio (Figure 2C) only increased significantly in the hyperglycemic cells incubated with WPF (30.9%).

The digested fractions also showed a regulatory effect on the NF-κB pathway in hyperglycemic cells (Figure 3). Under hyperglycemic conditions a significant increase were observed in the mRNA levels of NF-κB (26.5% increase compared to NG cells) (Figure 3A). No change was observed in cells treated with WPGI and a significant decrease was showed in the presence of the WPF fraction. The pIKKαβ/IKKαβ, pNF-κB p65/NF-κB p65 and pIκBα/IKBα ratios increased for the non-treated HG cells (3.43, 74.3 and 91.5%, with respect to NG cells) (Figures 3C, 3D and 3E, respectively). The treatment of HG cells with WPGI and WPF significantly reduced the levels of pIκBα/IκBα and pIKK/IKK. However, the pNF-κB p65/NF-κB p65 ratio significantly decreased following treatment with WPF and there was no significant decrease in the presence of WPGI.

The figure 4 showed the SIRT1 mRNA levels in hyperglycemic cells treated with the rWPP-digested fractions. A significant reduction of 1.80-fold in the HG cells was observed compared with the NG cells, and WPF produced a significant increase (1.34 fold) in the mRNA levels of SIRT1 with respect to the NG cells.

The cellular redox status was evaluated in hyperglycemic cells by analyzing the mRNA expression of the glutathione metabolism enzymes and the ratio of GSH/GSSG (Figure 5). In HG cells, the glutamate cysteine ligase (GCLC) mRNA levels (figure 5A) showed the most marked decrease (a 6.7-fold reduction in comparison with normoglycemic cells) compared with the enzymes glutathione synthetase (GS) (Figure 5B) and the glutathione reductase (GR) (Figure 5C) that decreased about 3.1 and 3.0-fold times. The HG cells treated with WPF increased significantly the mRNA levels of all three enzymes (8.1, 3.1 and 3.5-fold, respectively), and the WPGI only showed a significant increase for GS and GR (2.5 and 1.9-fold, respectively). The GSH/GSSG ratio was decreased by 46.3% under hyperglycemic conditions and the presence of WPGI and WPF in the medium significantly increased the ratio by 45.9% and 59.7 %, respectively (Figure 5D).

With regard to the enzymatic antioxidant system, the mRNA levels of SOD1, CAT, GPX1, HO1 and NQO1 (Figure 6A, 6B, 6C, 6D and 6E) were reduced (9.4, 5.0, 2.7, 2.9 and 2.9-fold, respectively) under hyperglycemic conditions in comparison with the normoglycemic cells and SOD1 showed the highest increase. Cell treatment with WPF increased the mRNA levels of all the antioxidant enzymes. However, cell treatment with WPGI only increased the mRNA of CAT, HO1 and NQO1, although no significant differences were observed for SOD1 and GPX1.

In contrast, the hyperglycemic treatment resulted in a higher increase (4.8 fold) of the mRNA levels of SOD2 (Figure 7A) and the presence of WPGI and WPF in the incubation medium decreased the mRNA levels of SOD2, which reached normoglycemic values. A similar effect was observed for the mRNA levels of COX2 and NOX4 (Figure 7B and 7C). Those two levels increased (2.7 and 2.0-fold, respectively) under hyperglycemic conditions and cell treatment with the rWPP-digested fractions significantly reduced the expression of both enzymes.

4 Discussion

In previous studies we have demonstrated that hyperglycemia induced oxidative stress in EA.hy926 endothelial cells after the evaluation of different parameters such as ROS and NO levels and cellular antioxidant systems (Del Pino-García, Gerardi, Rivero-Pérez, González-SanJosé, et al., 2016). Furthermore, we reported that a diet enriched with a product obtained from rWPP modulated hypertension and diabetes in rats (Del Pino-García, Rivero-Pérez, González-Sanjosé, et al., 2016; Del Pino-García et al., 2017). In this regard, with this study we evaluated the Nrf2 and NF-κB cross-talk as a mechanism involved in the hyperglycemic-induced oxidative stress observed previously in EA.hy926 endothelial cells.

4.1 Downregulation of Nrf2/ARE and upregulation of NF-κB pathways lead to an adaptive response of SOD2 in hyperglycemic endothelial cells

Hyperglycemia plays a crucial role in the development of endothelial dysfunction (Patel, Chen, Das, & Kavdia, 2013; Ungvari et al., 2011) due to an increase in the oxidative stress and inflammation (Patel et al., 2013) modulated by the transcription factors Nrf2 and NF-κB.

Nrf2, a key transcription factor of antioxidant gene expression, is regulated by kinases such as Akt and PKA/p38-MAPK (Eggler, 2013). In other hand, NF-κB modulates the proinflammatory gene expression and regulates the expression of the antioxidant enzyme SOD2 (Dhar & St, 2012; Kinugasa et al., 2015; Zelko, Mariani, & Folz, 2002). Furthermore, it is known that the presence of NF-κB binding sites in the promoter

region of the Nrf2 gene suggests cross-talk between these two regulators of inflammatory processes (Nair, Doh, Chan, Kong, & Cai, 2008; Wardyn, Ponsford, & Sanderson, 2015).

In this study, an opposite action of Nrf2 and NF-κB was observed under hyperglycemic conditions in cells. An increase in the expression of NF-κB is accompanied by an upregulated expression of the proinflammatory enzymes, NOX4 and COX2, and of the antioxidant enzyme SOD2. Likewise, a decreased expression of Nrf2 is accompanied by a downregulated expression of antioxidant enzymes (SOD1, GPX1, CAT, NQO1and HO1). These results suggested that the expression of SOD2 enzyme might to be consequence of the inflammation that occurs in hyperglycemic- cells. Therefore, this mechanism could be considered as an adaptive mechanism to hyperglycemia where NF-κB modulates the first cellular response to the oxidative injury and acts by increasing the levels of SOD2. It is well known that the expression of SOD2 is highly responsive to vascular oxidative stress and constitutes the predominant isoform of superoxide dismutase in the endothelial cell (Faraci & Didion, 2004). Furthermore, similar regulation was observed in other pathologies as tumor cells where an upregulation of SOD2 was dependent of inflammation-activated NF-κB (Kinugasa et al., 2015; Yi et al., 2017).

Furthermore, Nrf2 and NF-κB activities depend on the modulation by kinases such as Akt, PKA, PKC and MAPK that phosphorylate Nrf2 or NF-κB at specific sites and hyperglycemia impairment could promote endothelial cell proliferative dysfunction through PI3K-Akt signaling (Varma, 2005). In the present work, the downregulated Akt and p38-MAPK in the hyperglycemic cells could explain the lower levels of Nrf2 expression and pNrf2/Nrf2 ratio.

4.2 Upregulation of Nrf2/ARE and downregulation of NF-κB by rWPP

Dietary polyphenols, resveratrol and epigallocatechin-gallato, have been found to inhibit gene expression involved in the development and continuance of endothelial dysfunction through inactivation of the NF-κB pathway and /or activation of Nrf2 (Rahman, Biswas, & Kirkham, 2006; Son et al., 2010). In this study, the potentially bioavailable fractions of rWPP clearly attenuated hyperglycemic damage in endothelial cells, through Nrf2 and NF-κB signalling pathways. In this regard, WPGI and WPF treatments of hyperglycemic endothelial cells upregulated the Nrf2 pathway and downregulated the NF-κB pathway as showed the results of expression and phosphorylation of these two transcription factors.

The phosphorylation of Nrf2-serine 40, by protein kinase C, regulates its activity leading to the release of Nrf2 from its inhibitor and its translocation to the nucleus and to the activation of gene expression (Niture, Khatri, & Jaiswal, 2014; Zhang et al., 2018). Accordingly, the Nrf2 upregulation by the rWPP-digested

fractions stimulated the gene expression of antioxidant enzymes and inhibited inflammatory responses reducing the gene expression of COX2 and NOX4 and the antioxidant enzyme SOD2. However, the expression of NF-κB mRNA and the active phosphorylated form (pNFkB-p65) was reduced in the hyperglycemic cells treated with the rWPP-digested fractions, although it was only significantly for the WPF product. This reduction of NF-κB expression by WPF could be due to the content of phenolic acids such as hydroferulic acid (4.8 higher than in WPGI) as it is known to suppress NF-κB activation (Wang et al., 2016) and ferulic acid that decreases the phosphorylation of NF-κB under conditions of oxidative stress (Cao et al., 2015). Furthermore, the higher content of stilbenes in the WPF could to attenuate the phosphorylation, acetylation and nuclear translocation of NF-κB which is consistent with results of several studies (Chung et al., 2010; Shanmugam, Kannaiyan, & Sethi, 2011). On the other hand, the action mechanism of WPGI and WPF to decrease pNF-κB could be through the inhibition of NF-κB nuclear translocation and the transcription promotion of IκBα by modulation of the IKK/IκBα pathway. In this regard, it has been demonstrated that the phosphorylation of IKK and the subsequent degradation of IκBα can be inhibited in cells pre-treated with flavonols (Luo et al., 2015) such as observed in WPGI fraction. In addition, notable inhibition has been reported of IKK activation, IκBα degradation and NF-κB activation by epigallocatechin, a predominant flavan 3-ol of the WPF (Rahman et al., 2006).

The mechanisms through which the polyphenols could regulate the Nrf2 and NF-κB pathways in the hyperglycemic cells are as follows: (I) Nrf-2 and NF-κB activity might depend on the modulation exerted by several kinases such as Akt, PKA, PKC, MAPK that phosphorylate Nrf2 and NF-κB at specific sites; (II) The polyphenols might increase the expression of sirtuins (SIRT1 and SIRT2) that regulate the deacetylation of the NF-κB transcription factor, leading to a reduction of ROS and inflammatory cytokines. In addition, the inhibition of Nrf2 ubiquitination by SIRT1 might increase Nrf2 availability, favoring nuclear translocation of Nrf2 (K. Huang, Gao, & Wei, 2017); (III) The activator CBP complex is used by both transcription factors, thus an overexpression of Nrf2 induced by the polyphenols might limit the availability of CBP complexes for NF-κB (Wardyn et al., 2015).

Flavan-3-ols could activate a number of cellular kinases, including p38-MAPK and PI3K, which induce Nrf2 gene expression through PI3K/Akt and p38-MAPK pathways and the phosphorylation of Nrf2 through the activation of cAMP signalling by protein kinase A (PKA) (Bak, Jun, & Jeong, 2012). In this study, both the WPGI and the WPF fractions increased the levels of phosphorylated p38-MAPK and Akt in hyperglycemic endothelial cells, indicating a possible modulation of the Nrf2 pathway through these two kinases. Moreover,

it was reported that wine polyphenols caused a time-dependent phosphorylation of Akt, p38-MAPK and ERK1/2 that induced endothelium-dependent relaxations of coronary arteries, involving both nitric oxide and an endothelium-derived hyperpolarizing factor (Ndiaye, Chataigneau, Chataigneau, & Schini-Kerth, 2004). This regulation of p38-MAPK and Akt kinase phosphorylation by the digested fractions could to explain the observed in previous studies where the treatment of hyperglycemic cells with WPGI and WPF increased nitric oxide levels, but not the expression of the enzyme eNOS (Del Pino-García, Gerardi, Rivero-Pérez, González-SanJosé, et al., 2016).

NF-κB activation is also dependent on acetylation/deacetylation mediated by the sirtuins (SIRT1 and SIRT2) (Rahman et al., 2006). The marked decrease in SIRT1 gene expression, observed under hyperglycemic conditions, is probably attributed to the redox-sensitive property of SIRT1 (Chung et al., 2010) contributing to increased NF-κB activity. The role of WPF observed as activator of SIRT1 depends of their redox effect to decrease the NF-κB inflammatory responses and increased antioxidant enzymes by activation of the Nrf2 pathway (Bagul, Deepthi, Sultana, & Banerjee, 2015; Chung et al., 2010). Hence, this observation suggests that rWPP products contribute to prevention of endothelial dysfunction by increasing SIRT1 mRNA and protein levels, which in turn activate the Nrf2 pathway and, thereafter, attenuate both oxidative and inflammatory responses.

4.3 Modulation of downstream target genes: glutathione metabolism, antioxidants and inflammatory enzymes

The GSH/GSSG ratio was analyzed as a marker of the cell redox environment (Chen et al., 2013). The lower levels of the GSH/GSSG ratio observed in the hyperglycemic cells indicated an enhanced use of GSH or a decreased availability of NADPH under oxidative stress conditions. Hyperglycemic cells treated with the WPGI and WPF fractions improved the intracellular redox state with respect to the hyperglycemic enviromental. The metabolism of glutathione through GCLC, GS and GR activities plays a direct role in ROS scavenging and the regeneration of other antioxidants. The reduced expression of these enzymes in cells under hyperglycemic conditions is concordant with the observations of Powell et al. (2001). Furthermore, the action of the rWPP-digested fractions that increased the expression of those enzymes is consistent with the activation of the Nrf2/ARE and dowregulation of NF-κB pathways (Chen et al., 2013; Masella, Di Benedetto, Varì, Filesi, & Giovannini, 2005; Urata et al., 1996). Moreover, the rWPP-digested fractions also regulate the expression of antioxidant enzymes expression (SOD1, GPX1, CAT, HO1 and NQO1) by Nrf2/ARE pathway upregulated antioxidant gene expression, due to the presence of polyphenolic

compounds and their metabolites (Bagul et al., 2015; Chung et al., 2010; K. Huang et al., 2017). The WPF result in an increased of all enzymes expression but the WPGI treatment only increased CAT, HO1 and NQO1 expression. These results are in concordance with the different effect of both fractions on SIRT1 gene expression. In contrast, downregulation of NFkB by the WPGI and the WPF fractions in hypeglycemic cells, resulted in the decreased expression of inflammatory enzymes, NOX4 and COX2, possibly due to the presence of procyanidins (Surh et al., 2001) and phenolic acids such as ferulic acid (Lampiasi & Montana, 2017; Ndiaye et al., 2004). Interestingly, over-expression levels of SOD2 by hyperglycemia in endothelial cells induced by NF-κB, were downregulated by rWPP. Unlike the other antioxidant enzymes that are regulated by Nrf2, SOD2 genes have binding sites for NF-κB and other transcription factors that act in a cooperative manner through a transcription complex (Dhar & St, 2012).

5 Concluding remarks

The gastrointestinal and colonic fractions derived from the rWPP have shown potential protective effects against hyperglycemic-induced endothelial dysfunction and oxidative damage acting as inhibitors of proinflamatory proteins by downregulation of the NF-κB pathway and by increasing antioxidant enzymes through the upregulation of the Akt-p38-MAPK /Nrf2 pathways and regulation by deacetylasing SIRT1.

Moreover, our study has highlighted the early adaptive response of NF-κB/SOD2 under hyperglycemic conditions. On the contrary, cell treatment with the rWPP fractions decreased SOD2 gene expression through the downregulation of NF-κB and at the same time, increased the expression of the other antioxidant enzymes by upregulation of Nrf2.

This study has therefore provided evidence of the mechanisms that activate the protective effects of rWPP. These results form a solid foundation for future clinical studies, to understand its effects in greater detail and to take advantage of its benefits.

6 Conflicts of interest

The authors declare no conflict of interest.

7 Appendix: Supplementary material

Supplementary data to this article

8 Acknowledgments

The authors thank the financial support of the Autonomous Government of Castilla y León (Research project BU282U13).

9 Figure captions

Table 1. Phenolic Acids, stilbens, flavan-3-ols and flavonols composition of the digested fractions obtained from the red wine pomace product (rWPP) assessed by GC/MS/MS and by HPLC/DAD. WPGI: potentially bioavailable samples after *in vitro* gastrointestinal digestion; WPF potentially bioavailable samples after *in vitro* colonic fermentation. Data expressed as µg of compound /g of rWPP as mean values ± standard deviation (n = 3). Asterisk (*) indicate significant differences ($p<0.05$) between the WPGI and the WPF

Figure 1. Quantitative (qPCR) Nrf2 gene expression and Nrf2 Western blot analysis of normoglycemic (NG) or hyperglycaemic (HG) EA.hy926 treated with rWPP-digested fractions. (A) Relative expression of Nrf2 gene normalized to normoglycemic control cells (B) Bar graph of densitometry values of phosphorylated Nrf2 (pNrf2) expressed as fold change of total Nrf2. (C) Representative Western blots detecting β-actin, pNrf2 and Nrf2. Cells were treated with the potentially bioavailable compounds obtained after the in vitro gastrointestinal digestion (WPGI) or colonic fermentation (WPF) of the red wine pomace product (rWPP). mRNA levels of the Nrf2 under assessment were determined by quantitative real-time PCR (qPCR), normalized to the GAPDH gene expression. The western blot analysis was normalized to the β-actin expression. Data are presented as mean ± SD, n=3. Greek letters expressed significant differences ($p < 0.05$) among: normoglycemic cells (NG), hyperglycaemic cells (HG), WPGI-treated hyperglycaemic cells (WPGI) and WPF-treated hyperglycaemic cells (WPF).

Figure 2. Akt and p38-MAPK Western blot analysis of normoglycemic (NG) and hyperglycemic (HG) EA.hy926 treated with rWPP-digested fractions. (A) Representative Western blots detecting β-actin, p38-MAPK, phospho-p38-MAPK, Akt and pAkt (B) Bar graph of densitometry values of pAkt expressed as fold change of the total Akt. (C) Bar graph of densitometry values of phospho-p38-MAPK expressed as fold change of the total p38-MAPK. Cells were treated with the potentially bioavailable compounds obtained

after the *in vitro* gastrointestinal digestion (WPGI) or colonic fermented (WPF) of the red wine pomace product (rWPP). The western blot analysis was normalized to the β-actin expression. Data expressed as mean values ± standard deviation (n = 3). Greek letters expressed significant differences ($p < 0.05$) among: normoglycemic cells (NG), hyperglycaemic cells (HG), WPGI-treated hyperglycaemic cells (WPGI) and WPF-treated hyperglycaemic cells (WPF).

Figure 3. Quantitative (qPCR) NF-κB gene expression and NF-κB, IKKαβ and IκBα Western blot analysis of normoglycemic (NG) or hyperglycaemic (HG) EA.hy926 treated with rWPP-digested fractions. (A) Relative expression of NF-κB gene normalized to normoglycemic control cells (B) Representative Western blots detecting β-actin, NF-κB p65, pNF-κB p65, IKKαβ, p IKKαβ, IκBα and pIκBα (C) Bar graph of densitometry values of pIκBα expressed as fold change of total IκBα.(D) Bar graph of densitometry values of p IKKαβ expressed as fold change of total IKKαβ. (E) Bar graph of densitometry values of pNF-κB expressed as fold change of total NF-κB. Cells were treated with the potentially bioavailable compounds obtained after the in vitro gastrointestinal digestion (WPGI) or colonic fermentation (WPF) of the red wine pomace product (rWPP). mRNA levels under assessment were determined by quantitative real-time PCR (qPCR), normalized to the GAPDH gene expression. The western blot analysis was normalized to the β-actin expression. Data are presented as mean ± SD, n=3. Greek letters expressed significant differences ($p < 0.05$) among: normoglycemic cells (NG), hyperglycaemic cells (HG), WPGI-treated hyperglycaemic cells (WPGI) and WPF-treated hyperglycaemic cells (WPF).

Figure 4. Quantitative (qPCR) SIRT1 gene expression of normoglycemic (NG) or hyperglycaemic (HG) EA.hy926 treated with rWPP-digested fractions. Relative expression of SIRT1 gene normalized to normoglycemic control cells. Cells were treated with the potentially bioavailable compounds obtained after the in vitro gastrointestinal digestion (WPGI) or colonic fermentation (WPF) of the red wine pomace product (rWPP). mRNA levels of the SIRT1 under assessment were determined by quantitative real-time PCR (qPCR), normalized to the GAPDH gene expression. Data are presented as mean ± SD, n=3. Greek letters expressed significant differences ($p < 0.05$) among: normoglycemic cells (NG), hyperglycaemic cells (HG), WPGI-treated hyperglycaemic cells (WPGI) and WPF-treated hyperglycaemic cells (WPF).

Figure 5. Quantitative (qPCR) expression of the glutathione metabolism enzymes and redox status of normoglycemic (NG) or hyperglycaemic (HG) EA.hy926 treated with rWPP-digested fractions. Relative gene expression of GCLC (A), GS (B), and GR (C) normalized to normoglycemic control cells. Cellular redox status was assessed by the measurement of the GSH/GSSG ratio (D).Cells were treated with the potentially bioavailable compounds obtained after the in vitro gastrointestinal digestion (WPGI) or colonic fermentation (WPF) of the red wine pomace product (rWPP). mRNA levels under assessment were determined by quantitative real-time PCR (qPCR), normalized to the GAPDH gene expression. Data are presented as mean ± SD, n=3. Greek letters expressed significant differences ($p < 0.05$) among: normoglycemic cells (NG), hyperglycaemic cells (HG), WPGI-treated hyperglycaemic cells (WPGI) and WPF-treated hyperglycaemic cells (WPF).GCLC: glutamate-cysteine ligase catalytic subunit, GS: gluthatione synthase; GR: glutathione reductase and GSH/GSSG ratio: glutathione/glutathione disulfide ratio.

Figure 6. Quantitative (qPCR) antioxidant enzymes gene expression of normoglycemic (NG) or hyperglycaemic (HG) EA.hy926 treated with rWPP-digested fractions. Relative gene expression of SOD1 (A), CAT (B), GPX1(C), HO1(D) and NQO1 (E) normalized to normoglycemic control cells. Cells were treated with the potentially bioavailable compounds obtained after the in vitro gastrointestinal digestion (WPGI) or colonic fermention (WPF) of the red wine pomace product (rWPP). mRNA levels under assessment were determined by quantitative real-time PCR (qPCR), normalized to the GAPDH gene expression. Data are presented as mean ± SD, n=3. Greek letters expressed significant differences ($p < 0.05$) among: normoglycemic cells (NG), hyperglycaemic cells (HG), WPGI-treated hyperglycaemic cells (WPGI) and WPF-treated hyperglycaemic cells (WPF). SOD1: superoxide dismutase 1; CAT: catalase; GPX1: glutathione peroxidise 1; HO1: hemo oxygenase 1 and NQO1; NAD(P)H:quinone oxidoreductase 1.

Figure 7. Quantitative (qPCR) SOD2, COX2 and NOX4 gene expression of normoglycemic (NG) or hyperglycaemic (HG) EA.hy926 treated with rWPP-digested fractions. Relative gene expression of SOD2 (A), COX2 (B) and NOX4 (C) normalized to normoglycemic control cells. Cells were treated with the potentially bioavailable compounds obtained after the in vitro gastrointestinal digestion (WPGI) or colonic fermention (WPF) of the red wine pomace product (rWPP). mRNA levels under assessment were determined by quantitative real-time PCR (qPCR), normalized to the GAPDH gene expression. Data are presented as

mean ± SD, n=3. Greek letters expressed significant differences ($p < 0.05$) among: normoglycemic cells (NG), hyperglycaemic cells (HG), WPGI-treated hyperglycaemic cells (WPGI) and WPF-treated hyperglycaemic cells (WPF). SOD2: superoxide dismutase 2COX2: ciclooxigenase 2 and NOX4; NADPH oxidase 4.

9 References

Afrin, S., Giampieri, F., Gasparrini, M., Forbes-hernández, T. Y., Cianciosi, D., Reboredo-Rodriguez, P., Shang, K., Manna, P., Daglia, M., Atanasov, A.G., & Battino, M. (2018). Dietary phytochemicals in colorectal cancer prevention and treatment : A focus on the molecular mechanisms involved. Biotechnology Advances, (November), 1–38. https://doi.org/10.1016/j.biotechadv.2018.11.011

Bagul, P. K., Deepthi, N., Sultana, R., & Banerjee, S. K. (2015). Resveratrol ameliorates cardiac oxidative stress in diabetes through deacetylation of NFkB-p65 and histone 3. Journal of Nutritional Biochemistry (Vol. 26). Elsevier B.V. https://doi.org/10.1016/j.jnutbio.2015.06.006

Bak, M. J., Jun, M., & Jeong, W. S. (2012). Procyanidins from wild grape (Vitis amurensis) seeds regulate ARE-mediated enzyme expression via Nrf2 coupled with p38 and PI3K/Akt pathway in HepG2 cells. International Journal of Molecular Sciences, 13(1), 801–818. https://doi.org/10.3390/ijms13010801

Battino, M., Giampieri, F., Pistollato, F., Sureda, A., Roberto, M., de Oliveira, M. R., Pittalá, V., Fallarino, F., Navabi, S.F., Atanasov, G., & Navabi, S.M. (2018). Nrf2 as regulator of innate immunity : A molecular Swiss army knife ! Biotechnology Advances, 36(2), 358–370. https://doi.org/10.1016/j.biotechadv.2017.12.012

Cao, Y. jun, Zhang, Y. min, Qi, J. peng, Liu, R., Zhang, H., & He, L. chong. (2015). Ferulic acid inhibits H2O2-induced oxidative stress and inflammation in rat vascular smooth muscle cells via inhibition of the NADPH oxidase and NF-κB pathway. International Immunopharmacology, 28(2), 1018–1025. https://doi.org/10.1016/j.intimp.2015.07.037

Chen, F., Qian, L. H., Deng, B., Liu, Z. M., Zhao, Y., & Le, Y. Y. (2013). Resveratrol protects vascular endothelial cells from high glucose-induced apoptosis through inhibition of nadph oxidase activation-driven oxidative stress. CNS Neuroscience and Therapeutics, 19(9), 675–681. https://doi.org/10.1111/cns.12131

Chung, S., Yao, H., Caito, S., Hwang, J. woong, Arunachalam, G., & Rahman, I. (2010). Regulation of SIRT1 in cellular functions: Role of polyphenols. Archives of Biochemistry and Biophysics, 501(1),

79–90. https://doi.org/10.1016/j.abb.2010.05.003

Del Pino-García, R., Gerardi, G., Rivero-Pérez, M. D., González-SanJosé, M. L., García-Lomillo, J., & Muñiz, P. (2016). Wine pomace seasoning attenuates hyperglycaemia-induced endothelial dysfunction and oxidative damage in endothelial cells. Journal of Functional Foods, 22, 431–445. https://doi.org/10.1016/j.jff.2016.02.001

Del Pino-García, R., González-Sanjosé, M. L., Rivero-Pérez, M. D., García-Lomillo, J., & Muñiz, P. (2016). Total antioxidant capacity of new natural powdered seasonings after gastrointestinal and colonic digestion. Food Chemistry, 211, 707–714. https://doi.org/10.1016/j.foodchem.2016.05.127

Del Pino-García, R., Rivero-Pérez, M. D., González-Sanjosé, M. L., Castilla-Camina, P., Croft, K. D., & Muñiz, P. (2016). Attenuation of oxidative stress in Type 1 diabetic rats supplemented with a seasoning obtained from winemaking by-products and its effect on endothelial function. Food and Function, 7(10), 4410–4421. https://doi.org/10.1039/c6fo01071g

Del Pino-García, R., Rivero-Pérez, M. D., González-SanJosé, M. L., Croft, K. D., & Muñiz, P. (2016). Bioavailability of phenolic compounds and antioxidant effects of wine pomace seasoning after oral administration in rats. Journal of Functional Foods, 25(2), 486–496. https://doi.org/10.1016/j.jff.2016.06.030

Del Pino-García, R., Rivero-Pérez, M. D., González-SanJosé, M. L., Croft, K. D., & Muñiz, P. (2017). Antihypertensive and antioxidant effects of supplementation with red wine pomace in spontaneously hypertensive rats. Food & Function, 8(7), 2444–2454. https://doi.org/10.1039/C7FO00390K

Dhar, S. K., & St, D. K. (2012). Free Radical Biology and Medicine Manganese superoxide dismutase regulation and cancer. Free Radical Biology and Medicine, 52(11–12), 2209–2222. https://doi.org/10.1016/j.freeradbiomed.2012.03.009

Eggler, A. L. (2013). Chemical and biological mechanisms of phytochemical activation of Nrf2 and importance in disease prevention Aimee (Vol. 43). https://doi.org/https//doi.org/doi:10.1007/978-3-319-00581-2_7

Faraci, F. M., & Didion, S. P. (2004). Vascular protection: Superoxide dismutase isoforms in the vessel wall. Arteriosclerosis, Thrombosis, and Vascular Biology, 24(8), 1367–1373. https://doi.org/10.1161/01.ATV.0000133604.20182.cf

García-Lomillo, J., González-SanJosé, M. L., Del Pino-García, R., Rivero-Pérez, M. D., & Muñiz-Rodríguez, P. (2014). Antioxidant and antimicrobial properties of wine byproducts and their potential

uses in the food industry. Journal of Agricultural and Food Chemistry, 62(52), 12595–12602. https://doi.org/10.1021/jf5042678

Gopalakrishnan, A., & Tony Kong, A. N. (2008). Anticarcinogenesis by dietary phytochemicals: Cytoprotection by Nrf2 in normal cells and cytotoxicity by modulation of transcription factors NF-κB and AP-1 in abnormal cancer cells. Food and Chemical Toxicology, 46(4), 1257–1270. https://doi.org/10.1016/j.fct.2007.09.082

Huang, H., Nguyen, T., & Pickett, C. B. (2002). Phosphorylation of Nrf2 at Ser-40 by Protein Kinase C Regulates Antioxidant Response Element-mediated Transcription. The Journal of Biological Chemistry, 277(45), 42769–42774. https://doi.org/10.1074/jbc.M206911200

Huang, K., Gao, X., & Wei, W. (2017). The crosstalk between Sirt1 and Keap1/Nrf2/ARE anti-oxidative pathway forms a positive feedback loop to inhibit FN and TGF-β1 expressions in rat glomerular mesangial cells. Experimental Cell Research, 361(1), 63–72. https://doi.org/10.1016/j.yexcr.2017.09.042

Kinugasa, H., Whelan, K. A., Tanaka, K., Natsuizaka, M., Long, A., Guo, A., Chang, S., Kagawa, S., Srinivasan, S., Gua, M., Yamamoto, K, Avadhani, N.G., Alan, J., Nakawaga, H., & Carolina, S. (2015). Mitochondrial SOD2 regulates epithelial-mesenchymal transition and cell populations defined by differential CD44 expression. Oncogene, 34(41), 5229–5239. https://doi.org/10.1038/onc.2014.449.Mitochondrial

Lakshminarasimhan, M., Rauh, D., Schutkowski, M., & Steegborn, C. (2013). Sirt1 activation by resveratrol is substrate sequence-selective. Aging, 5(3), 151–154. https://doi.org/10.18632/aging.100542

Lampiasi, N., & Montana, G. (2017). An in vitro inflammation model to study the Nrf2 and NF-κB crosstalk in presence of ferulic acid as modulator. Immunobiology, 223(4–5), 349–355. https://doi.org/10.1016/j.imbio.2018.07.022

Luo, C., Yang, H., Tang, C., Yao, G., Kong, L., He, H., & Zhou, Y. (2015). Kaempferol alleviates insulin resistance via hepatic IKK/NF-κB signal in type 2 diabetic rats. International Immunopharmacology, 28(1), 744–750. https://doi.org/10.1016/j.intimp.2015.07.018

Masella, R., Di Benedetto, R., Varì, R., Filesi, C., & Giovannini, C. (2005). Novel mechanisms of natural antioxidant compounds in biological systems: Involvement of glutathione and glutathione-related enzymes. Journal of Nutritional Biochemistry, 16(10), 577–586. https://doi.org/10.1016/j.jnutbio.2005.05.013

Nair, S., Doh, S. T., Chan, J. Y., Kong, A. N., & Cai, L. (2008). Regulatory potential for concerted modulation of Nrf2- and Nfkb1-mediated gene expression in inflammation and carcinogenesis. British Journal of Cancer, 99(12), 2070–2082. https://doi.org/10.1038/sj.bjc.6604703

Ndiaye, M., Chataigneau, T., Chataigneau, M., & Schini-Kerth, V. B. (2004). Red wine polyphenols induce EDHF-mediated relaxations in porcine coronary arteries through the redox-sensitive activation of the PI3-kinase/Akt pathway. British Journal of Pharmacology, 142(7), 1131–1136. https://doi.org/10.1038/sj.bjp.0705774

Niture, S. K., Khatri, R., & Jaiswal, A. K. (2014). Free Radical Biology and Medicine, 66, 36–44. https://doi.org/10.1016/j.freeradbiomed.2013.02.008

Patel, H., Chen, J., Das, K. C., & Kavdia, M. (2013). Hyperglycemia induces differential change in oxidative stress at gene expression and functional levels in HUVEC and HMVEC. Cardiovascular Diabetology, 12(1), 1–14. https://doi.org/10.1186/1475-2840-12-142

Pedruzzi, L. M., Stockler-Pinto, M. B., Leite, M., & Mafra, D. (2012). Nrf2-keap1 system versus NF-κB: The good and the evil in chronic kidney disease? Biochimie, 94(12), 2461–2466. https://doi.org/10.1016/j.biochi.2012.07.015

Pérez-Magariño, S., Ortega-Heras, M., & Cano-Mozo, E. (2008). Optimization of a solid-phase extraction method using copolymer sorbents for isolation of phenolic compounds in red wines and quantification by HPLC. Journal of Agricultural and Food Chemistry, 56(24), 11560–11570. https://doi.org/10.1021/jf802100j

Powell, L. A., Nally, S. M., McMaster, D., Catherwood, M. A., & Trimble, E. R. (2001). Restoration of glutathione levels in vascular smooth muscle cells exposed to high glucose conditions. Free Radical Biology and Medicine, 31(10), 1149–1155.

Rahman, I., Biswas, S. K., & Kirkham, P. A. (2006). Regulation of inflammation and redox signaling by dietary polyphenols. Biochemical Pharmacology, 72(11), 1439–1452. https://doi.org/10.1016/j.bcp.2006.07.004

Scalbert, A., & Williamson, G. (2000). Chocolate : Modern Science Investigates an Ancient Medicine Dietary Intake and Bioavailability of Polyphenols 1. The Journal of Nutrition, 130((8S Suppl)), 2073–2085. https://doi.org/10.1089/109662000416311

Shanmugam, M. K., Kannaiyan, R., & Sethi, G. (2011). Targeting cell signaling and apoptotic pathways by dietary agents: Role in the prevention and treatment of cancer. Nutrition and Cancer, 63(2), 161–173.

https://doi.org/10.1080/01635581.2011.523502

Son, P. S., Park, S. A., Na, H. K., Jue, D. M., Kim, S., & Surh, Y. J. (2010). Piceatannol, a catechol-type polyphenol, inhibits phorbol ester-induced NF-κB activation and cyclooxygenase-2 expression in human breast epithelial cells: Cysteine 179 of IKKβ as a potential target. Carcinogenesis, 31(8), 1442–1449. https://doi.org/10.1093/carcin/bgq099

Surh, Y. J., Chun, K. S., Cha, H. H., Han, S. S., Keum, Y. S., Park, K. K., & Lee, S. S. (2001). Molecular mechanisms underlying chemopreventive activities of anti-inflammatory phytochemicals: Down-regulation of COX-2 and iNOS through suppression of NF-κB activation. Mutation Research - Fundamental and Molecular Mechanisms of Mutagenesis, 480–481, 243–268. https://doi.org/10.1016/S0027-5107(01)00183-X

Twentyman, P. R., & Luscombe, M. (1987). A study of some variables in a tetrazolium dye (MTT) based assay for cell growth and chemosensitivity. British Journal of Cancer, 56(3), 279–285. https://doi.org/10.1038/bjc.1987.190

Ungvari, Z., Bailey-Downs, L., Gautam, T., Jimenez, R., Losonczy, G., Zhang, C., Ballabh, P., Recchia, F.A., Wilkerson, D.C., Songtag, W.E., Pearson, K., de Cabo, R., & Csiszar, A. (2011). Adaptive induction of NF-E2-related factor-2-driven antioxidant genes in endothelial cells in response to hyperglycemia. American Journal of Physiology-Heart and Circulatory Physiology, 300(4), H1133–H1140. https://doi.org/10.1152/ajpheart.00402.2010

Urata, Y., Yamamoto, H., Goto, S., Tsushima, H., Akazawa, S., Yamashita, S., Nagataki, S., & Kondo, T. (1996). Long exposure to high glucose concentration impairs the responsive expression of gamma-glutamylcysteine synthetase by interleukin-1beta and tumor necrosis factor-alpha in mouse endothelial cells. The Journal of Biological Chemistry, 271(25), 15146–15152.

Varma, S. (2005). Hyperglycemia alters PI3k and Akt signaling and leads to endothelial cell proliferative dysfunction. AJP: Heart and Circulatory Physiology, 289(4), H1744–H1751. https://doi.org/10.1152/ajpheart.01088.2004

Wang, Y., Huo, Y., Zhao, L., Lu, F., Wang, O., Yang, X., Ji, B., & Zhou, F. (2016). Cyanidin-3-glucoside and its phenolic acid metabolites attenuate visible light-induced retinal degeneration in vivo via activation of Nrf2/HO-1 pathway and NF-κB suppression. Molecular Nutrition and Food Research, 60(7), 1564–1577. https://doi.org/10.1002/mnfr.201501048

Wardyn, J. D., Ponsford, A. H., & Sanderson, C. M. (2015). Dissecting molecular cross-talk between Nrf2

and NF-κB response pathways. Biochemical Society Transactions, 43(4), 621–626. https://doi.org/10.1042/BST20150014

Yeung, F., Hoberg, J. E., Ramsey, C. S., Keller, M. D., Jones, D. R., Frye, R. A., & Mayo, M. W. (2004). Modulation of NF-κB-dependent transcription and cell survival by the SIRT1 deacetylase. EMBO Journal, 23(12), 2369–2380. https://doi.org/10.1038/sj.emboj.7600244

Yi, L., Shen, H., Zhao, M., Shao, P., Liu, C., Cui, J., Wang, J., Wang, C., Guo, N., Kang, L., Lw, O., Xing, L., & Zhang, X. (2017). Inflammation-mediated SOD-2 upregulation contributes to epithelial-mesenchymal transition and migration of tumor cells in aflatoxin G1-induced lung adenocarcinoma. Scientific Reports, 7(1), 1–13. https://doi.org/10.1038/s41598-017-08537-2

Zhang, H., Yuan, B., Huang, H., Qu, S., Yang, S., & Zeng, Z. (2018). Brazilian Journal of Medical and Biological Research, 51(10), 1–10. https://doi.org/10.1590/1414-431X20187439

Zelko, I. N., Mariani, T. J., & Folz, R. J. (2002). Superoxide dismutase multigene family: a comparison of the CuZn-SOD (SOD1), Mn-SOD (SOD2), AND EC-SOD (SOD3) gene structures, evolution, and expression. Free Radical Biology and Medicine, 33(3), 337–349. https://doi.org/10.1017/S0952675714000244

Table

Table 1.

	Content (µg per g rWPP)		
	WPGI	WPF	
Phenolic acids			
Hydroxybenzoic acids			
meta-Hydroxyphenylacetic acid	5.09 ± 1.15	13.5 ± 2	*
para-Hydroxyphenylacetic acid	22,0 ± 7.2	16.2 ± 4.1	
Vanillic acid	9.14 ± 1.62	11.3 ± 2.8	
Homovanillic acid	2.67 ± 0.17	2.72 ± 0.08	
Protocatechuic acid	26.4 ± 10.5	11.3 ± 4.3	
Homoprotocatechuic acid	24 ± 3.4	45.1 ± 10.9	
Gentisic acid	37 ± 4.4	53.1 ± 4.55	*
Syringic acid	14.2 ± 4	4.33 ± 2.09	
4-O-methylgallic acid	1.7 ± 0.57	1.65 ± 0.28	
3-O-methylgallic acid	16.7 ± 6.9	27.1 ± 6.3	*
Total Hybroxybenzoic acids	*159 ± 11*	*186 ± 27*	
Hydroxycinnamic acids			
Dihydro-3-coumaric acid	1.82 ± 0.19	16.5 ± 4.7	*
Hydroferulic acid	2.86 ± 0.39	13.6 ± 3.6	*
Hydrocaffeic acid	10.1 ± 0.35	10.6 ± 0.5	
Isoferulic acid	3.8 ± 0.35	5.47 ± 0.37	
trans-Ferulic acid	10.5 ± 4.4	26.5 ± 11	
trans-Caffeic acid	13.1 ± 1.6	16.5 ± 1.11	
Total Hydroxycinnamic acids	*42.2 ± 5.8*	*89.1 ± 15.8*	*
TOTAL PHENOLIC ACIDS	**201 ± 16**	**275 ± 42**	*****
Stilbenes			
trans-piceid	0.16 ± 0.01	0.14 ± 0.01	
Resveratrol	0.73 ± 0.01	1.37 ± 0.13	*
TOTAL STILBENES	**0.9 ± 0.02**	**1.5 ± 0.13**	*****
Flavan-3-ols			
Flavan-3-ols (monomers)			
Catechin	17.6 ± 3.31	19.7 ± 0.48	
Epigallocatechin	19.9 ± 4.56	43.2 ± 2.14	*
Epicatechin	142 ± 13.4	132 ± 28	
Total Flavan-3-ols (monomers)	*180 ± 7*	*195 ± 30*	
Flavan-3-ols (dimers)			
Procyanidin B1	36.3 ± 0.01	130 ± 12	*
Procyanidin B2	9.6 ± 0.01	7.68 ± 1.59	
Total Flavan-3-ols (dimers)	*45.9 ± 0.01*	*138 ± 9*	*
TOTAL FLAVAN-3-OLS	**226 ± 7**	**333 ± 33**	*****
Flavonols			
Flavonol-3-O-glycosides			
Myricetin-3-O-rhamnoside	39.2 ± 1.54	ND	*
Kaempferol-3-O-rutinoside	81.6 ± 11	12.5 ± 0.01	*
Kaempferol-3-O-glucoside	ND	ND	
Quercetin-3-O-rutinoside	ND	ND	
TOTAL FLAVONOLS	**121 ± 10**	**12.5 ± 0.01**	*****

Table 1. Composition of the seedless red wine pomace product (rWPP)

Nutrient/Compound	Content (per 100 g rWPP)
Moisture (mL)	6.93 ± 2.26
Total fat (g)	4.7 ± 1.6
Total protein (g)	14.1 ± 1.9
Ash (g)	6.36 ± 1.01
Minerals (g)	
Potassium	2.33 ± 0.69
Sodium	0.055 ± 0.006
Calcium	0.340 ± 0.148
Total anthocyanins (g Malv-3GE)	0.268 ± 0.220
Total proanthocyanidins (g P-B1E)	4.181 ± 3.579
Total catechins (g D-CatE)	3.306 ± 0.110

Content expressed as mean values ± standard deviation (n=3)

Table 2. Antioxidant capacity of the seedless red wine pomace product (rWPP)

	Undigested	WPGI	WPF
Q-ABTS (mmol TE)	15.8 ± 1.5[a]	19.5 ± 0.1[b]	40.0 ± 8.3[c]
Q-FRAP (mmol Fe(II)E)	38.5 ± 0.3[b]	3.3 ± 0.1[a]	3.2 ± 0.2[a]

Content expressed as mean values ± standard deviation (n=3)

Table 3. Sequences of primer sets

	Primer Forward (5´- 3´)	Primer Reverse (5´- 3´)
GAPDH	GCTCTCCAGAACATCATCCC	GTCCACCACTGACACGTTG
CAT	TACGTCCTGAGTCTCTGCAT	CCCCATTTGCATTAACCAGC
COX2	CGGTGAAACTCTGGCTAGAC	GGGACTTGAGGAGGGTAGAT
GCLC	TGCAGTGGTGGATGGTTG	ATCAGTCCAGGAAACACACC
GPX1	CAGTTTGGGCATCAGGAGGAA	TCGAAGAGCATGAAGTTGGG
GR	TTTACCCCGATGTATCACGC	TTTCATCACACCCAAGTCCC
GS	CTGGTGCTACTGATTGCTCA	TCCAGAGACCCCTTTTCAGA
HO1	GCCAGCAACAAAGTGCAAG	AAAGCTGAGTGTAAGGACCC
NF-κB	GGCGAGAGGAGCACAGATAC	CTGATAGCCTGCTCCAGGTC
NOX4	GGAAGAGCCCAGATTCCAAG	AGTCTTTCGGCACAGTACAG
NQO1	GAAGAAAGGATGGGAGGTGG	GAACAGACTCGGCAGGATAC
Nrf2	ACCCTTGTCACCATCTCAGG	CAGGGAATGGGATATGGAGA
SIRT1	TCAGTGGCTGGAACAGTGAG	AGCGCCATGGAAAATGTAAC
SOD1	GGCCAAAGGATGAAGAGAGC	TGATGCAATGGTCTCCTGAG
SOD2	GGAACGGGGACACTTACAAA	ACTGAAGGTAGTAAGCGTGC

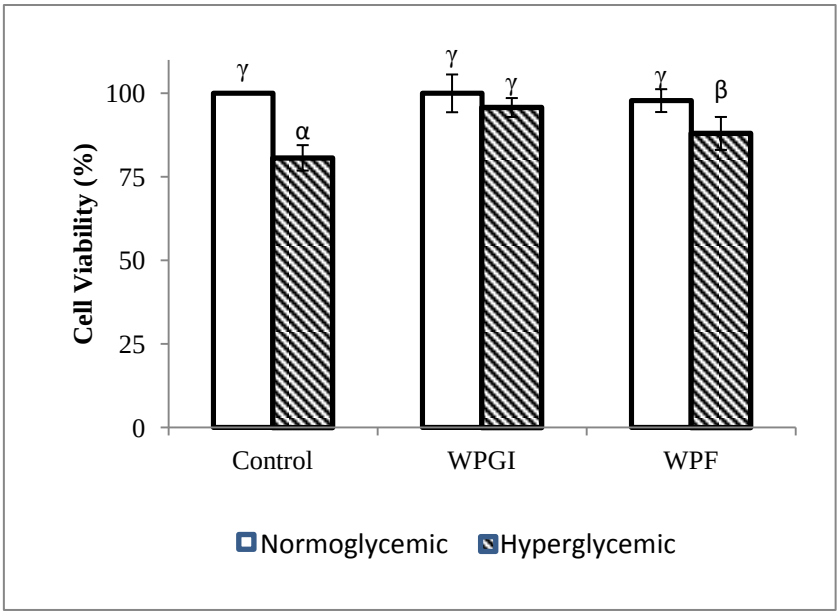

Figure 1 Supplementary Material. Cell viability of normoglycemic and hyperglycemic EA.hy926 endothelial cells treated with digested fractions obtained from the red wine pomace product (rWPP). WPGI: potentially bioavailable samples after *in vitro* gastrointestinal digestion; WPF potentially bioavailable samples after *in vitro* colonic fermentation; Control: Cells incubated under normoglycemis or hyperglycemic conditions in absence of the rWPP. Data expressed in % as mean values ± standard deviation (n = 3) with respect to the normoglycemic control cells (100%). Significant changes ($p<0.05$) between the control, the WPGI and the WPF treated cells are expressed in Greek letters.

Figure

Click here to download Figure: Figures.docx

Figure 1

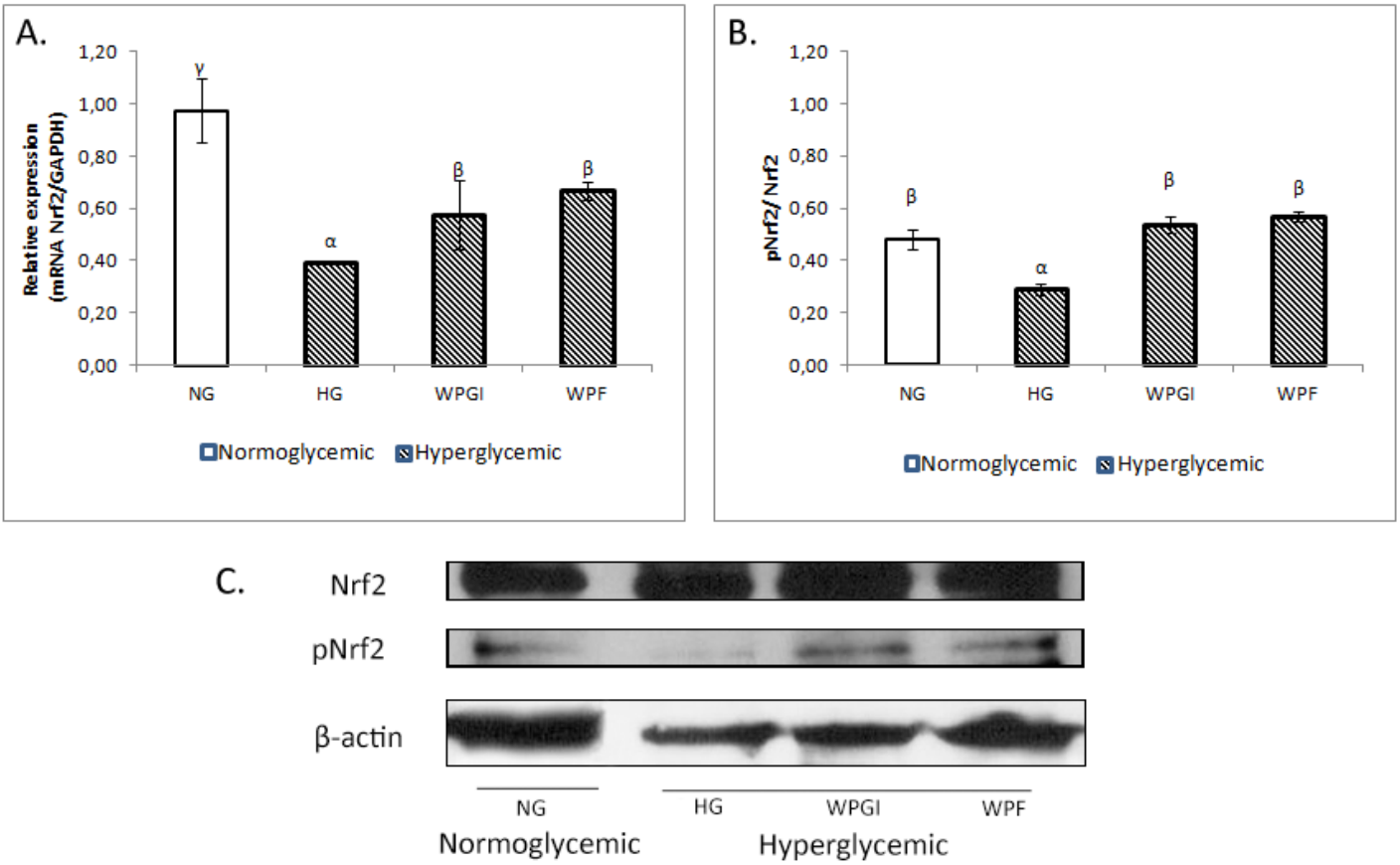

Figure 2

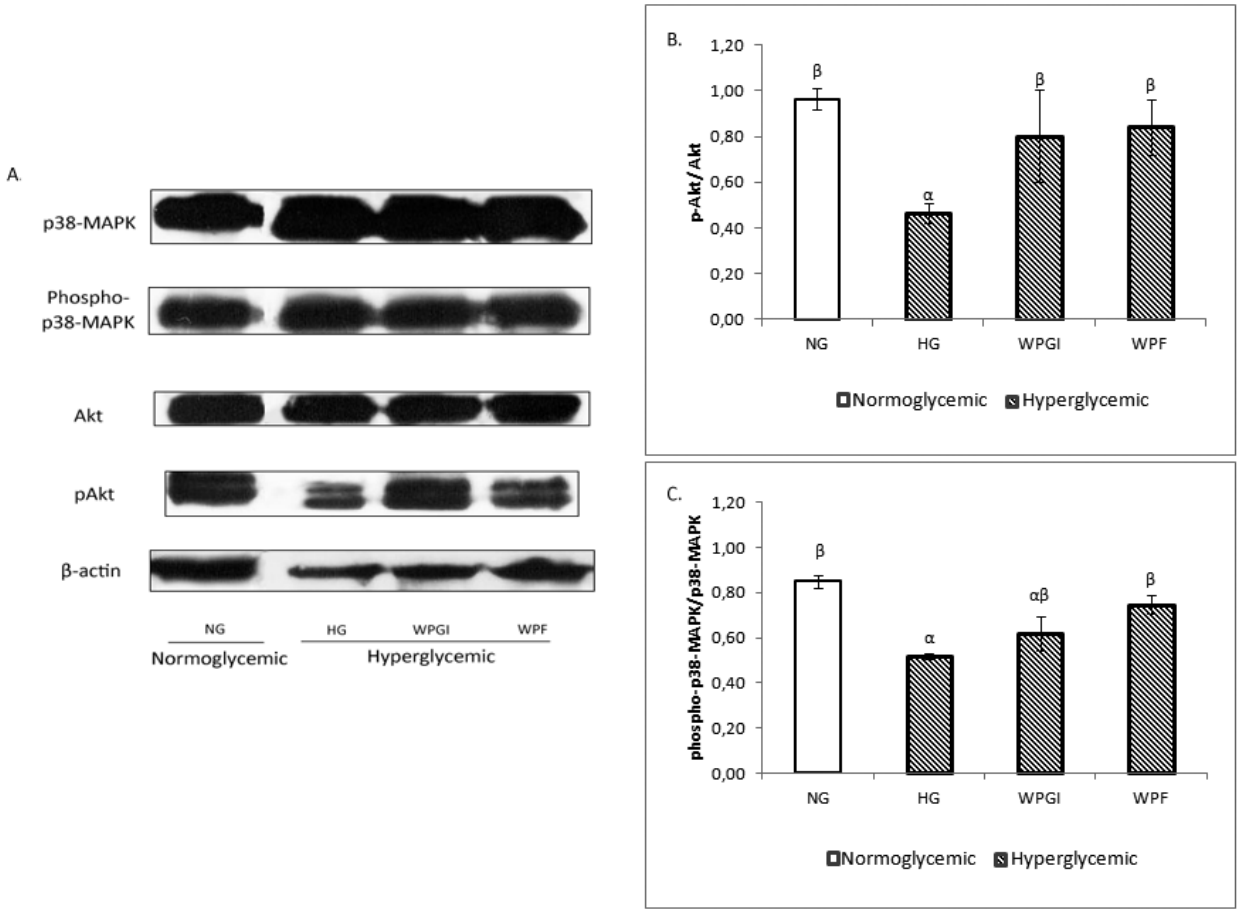
A.
p38-MAPK
Phospho-p38-MAPK
Akt
pAkt
β-actin
NG
HG
WPGI
WPF
Normoglycemic
Hyperglycemic
B.
p-Akt/Akt
1,20
1,00
0,80
0,60
0,40
0,20
0,00
β
α
β
β
NG
HG
WPGI
WPF
Normoglycemic
Hyperglycemic
C.
phospho-p38-MAPK/p38-MAPK
1,20
1,00
0,80
0,60
0,40
0,20
0,00
β
α
αβ
β
NG
HG
WPGI
WPF
Normoglycemic
Hyperglycemic

Figure 3

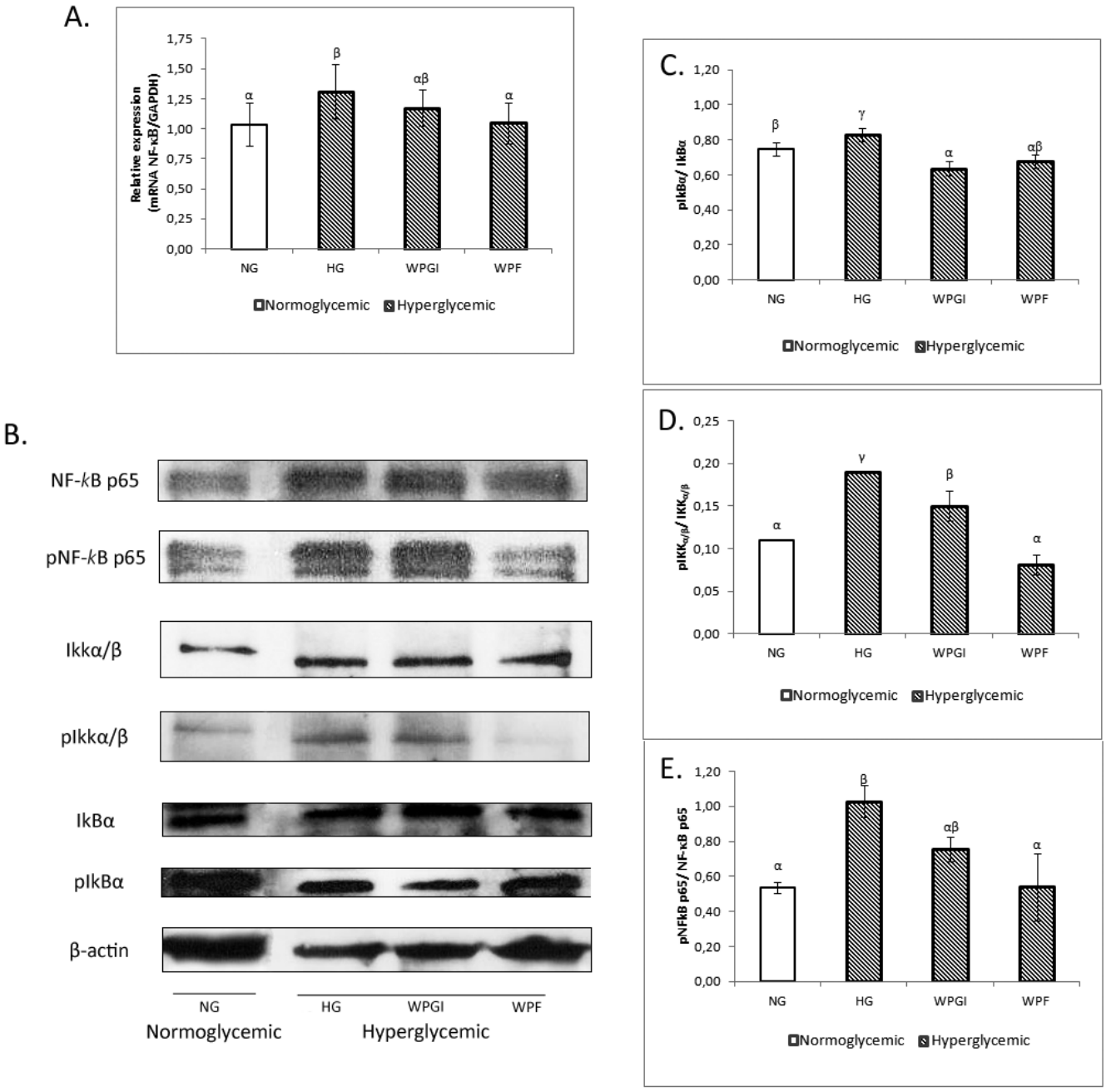
A.
Relative expression (mRNA NF-κB/GAPDH)
1,75
1,50
1,25
1,00
0,75
0,50
0,25
0,00
α
β
αβ
α
NG
HG
WPGI
WPF
Normoglycemic
Hyperglycemic
B.
NF-kB p65
pNF-kB p65
Ikkα/β
pIkkα/β
IkBα
pIkBα
β-actin
NG
HG
WPGI
WPF
Normoglycemic
Hyperglycemic
C.
pIkBα/ IkBα
1,20
1,00
0,80
0,60
0,40
0,20
0,00
β
γ
α
αβ
NG
HG
WPGI
WPF
Normoglycemic
Hyperglycemic
D.
pIKKα/β/ IKKα/β
0,25
0,20
0,15
0,10
0,05
0,00
α
γ
β
α
NG
HG
WPGI
WPF
Normoglycemic
Hyperglycemic
E.
pNFkB p65/ NF-κB p65
1,20
1,00
0,80
0,60
0,40
0,20
0,00
α
β
αβ
α
NG
HG
WPGI
WPF
Normoglycemic
Hyperglycemic

Figure 4

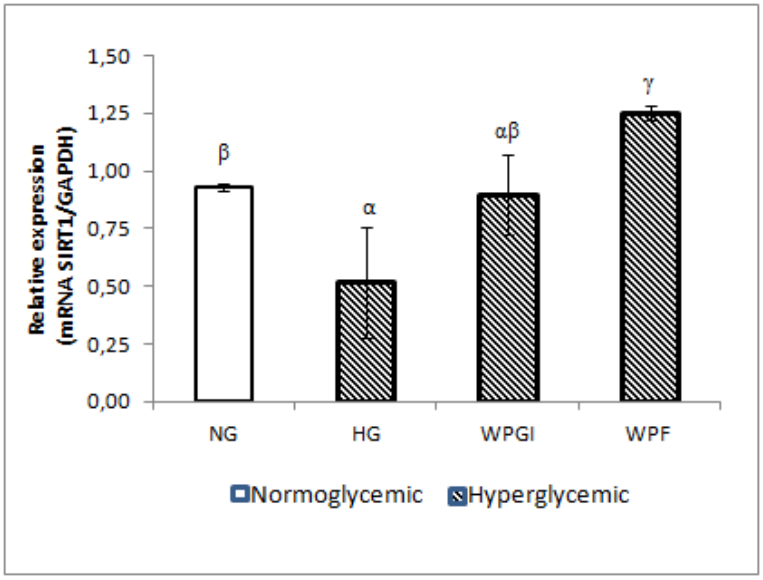
Relative expression (mRNA SIRT1/GAPDH)
1,50
1,25
1,00
0,75
0,50
0,25
0,00
β
α
αβ
γ
NG
HG
WPGI
WPF
Normoglycemic
Hyperglycemic

Figure 5

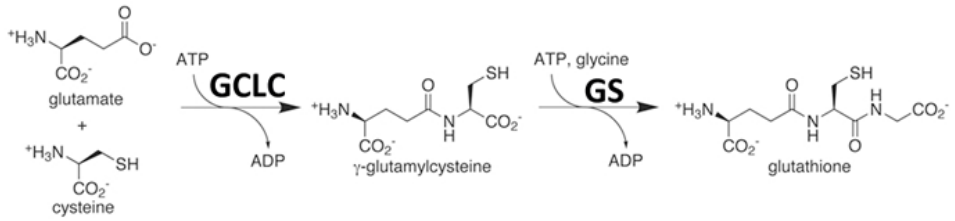
glutamate
cysteine
ATP
GCLC
ADP
γ-glutamylcysteine
ATP, glycine
GS
ADP
glutathione

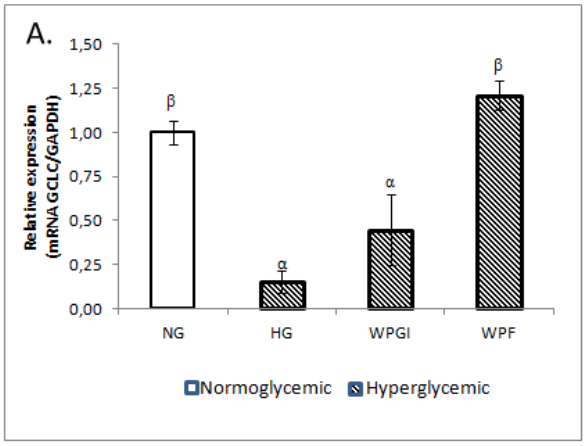
A.
Relative expression (mRNA GCLC/GAPDH)
1,50
1,25
1,00
0,75
0,50
0,25
0,00
β
α
β
α
NG
HG
WPGI
WPF
Normoglycemic
Hyperglycemic

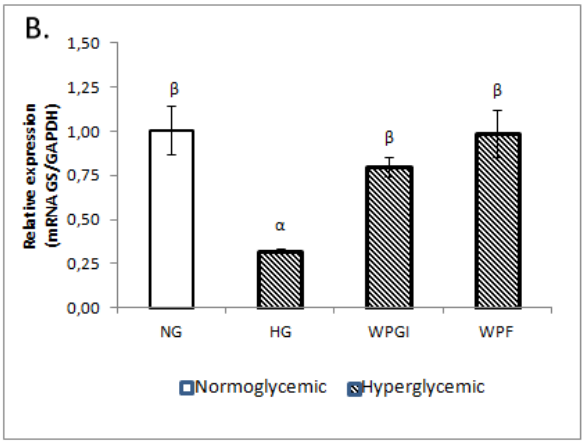
B.
Relative expression (mRNA GS/GAPDH)
1,50
1,25
1,00
0,75
0,50
0,25
0,00
β
α
β
β
NG
HG
WPGI
WPF
Normoglycemic
Hyperglycemic


Glutathione disulfide (GSSG)
GR
Glutathione (GSH)

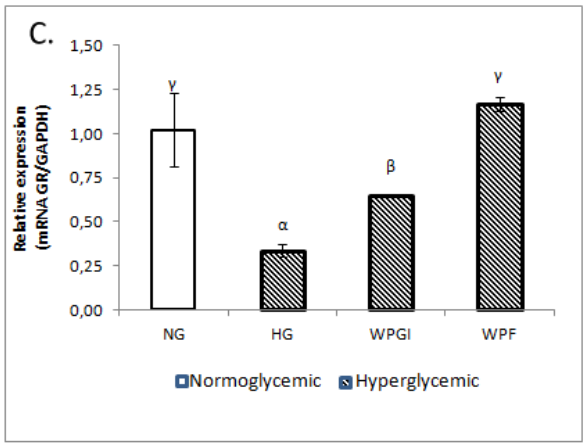
C.
Relative expression (mRNA GR/GAPDH)
1,50
1,25
1,00
0,75
0,50
0,25
0,00
γ
α
β
γ
NG
HG
WPGI
WPF
Normoglycemic
Hyperglycemic

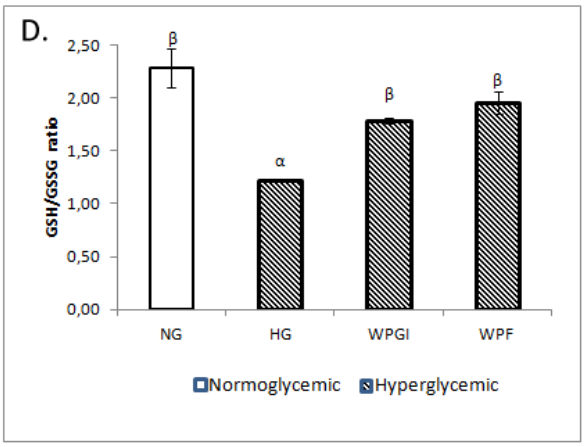
D.
GSH/GSSG ratio
2,50
2,00
1,50
1,00
0,50
0,00
β
α
β
β
NG
HG
WPGI
WPF
Normoglycemic
Hyperglycemic

Figure 6

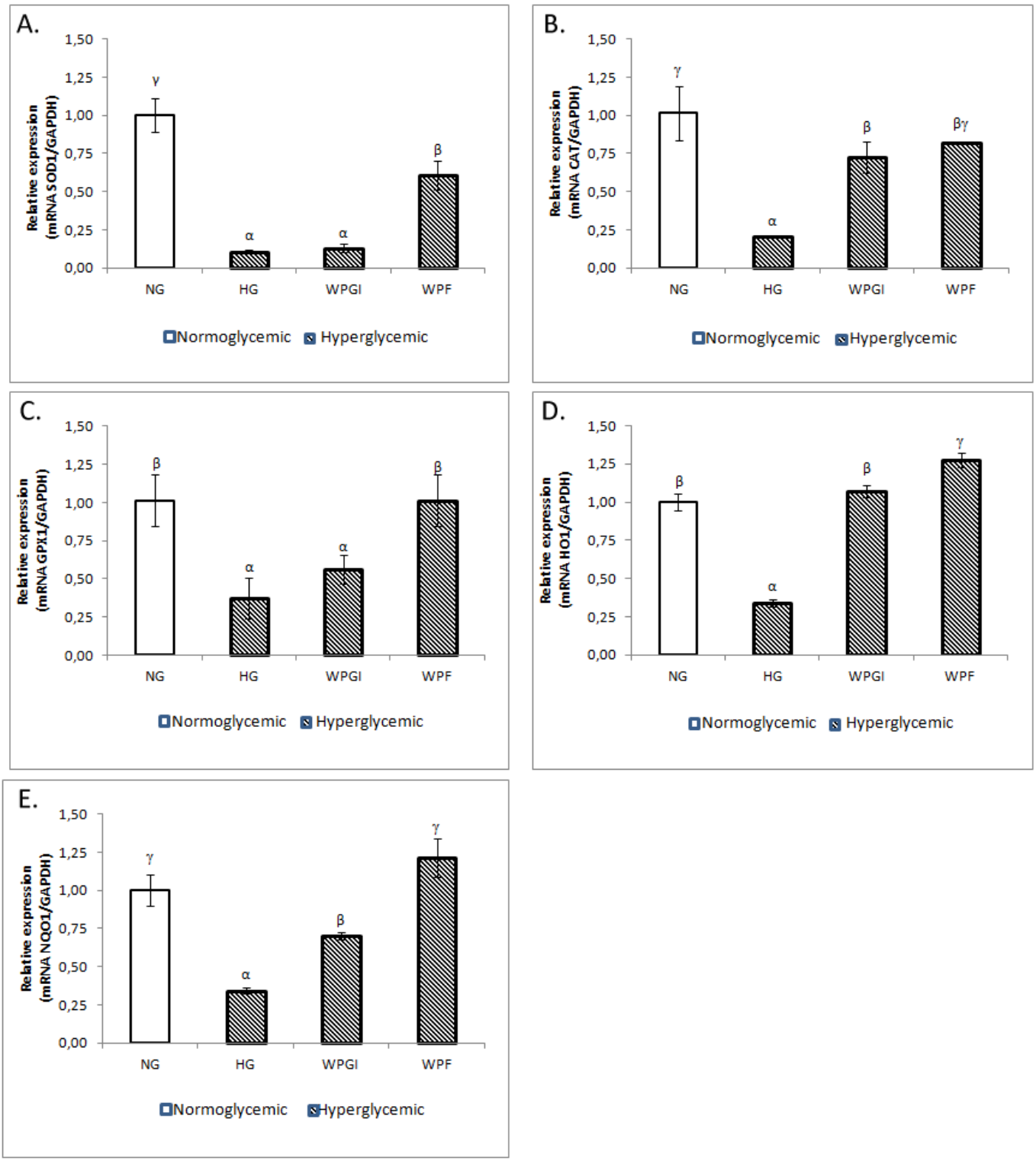
A.
Relative expression (mRNA SOD1/GAPDH)
1,50
1,25
1,00
0,75
0,50
0,25
0,00
γ
α
α
β
NG
HG
WPGI
WPF
Normoglycemic
Hyperglycemic
B.
Relative expression (mRNA CAT/GAPDH)
γ
α
β
βγ
C.
Relative expression (mRNA GPX1/GAPDH)
β
α
α
β
D.
Relative expression (mRNA HO1/GAPDH)
β
α
β
γ
E.
Relative expression (mRNA NQO1/GAPDH)
γ
α
β
γ

Figure 7

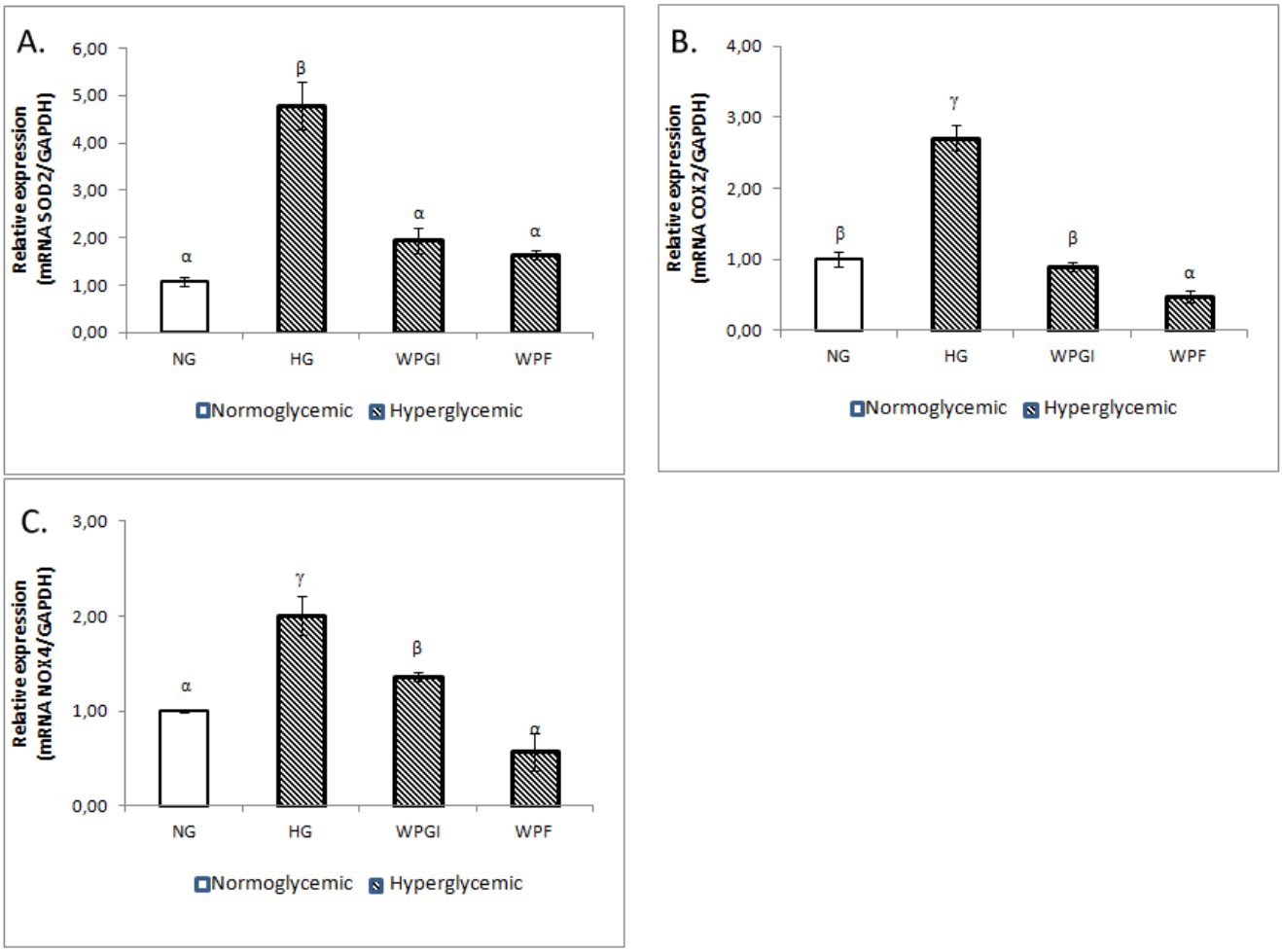
A.
Relative expression (mRNA SOD2/GAPDH)
6,00
5,00
4,00
3,00
2,00
1,00
0,00
α
β
α
α
NG
HG
WPGI
WPF
Normoglycemic
Hyperglycemic
B.
Relative expression (mRNA COX2/GAPDH)
4,00
3,00
2,00
1,00
0,00
β
γ
β
α
NG
HG
WPGI
WPF
Normoglycemic
Hyperglycemic
C.
Relative expression (mRNA NOX4/GAPDH)
3,00
2,00
1,00
0,00
α
γ
β
α
NG
HG
WPGI
WPF
Normoglycemic
Hyperglycemic

*Graphical Abstract

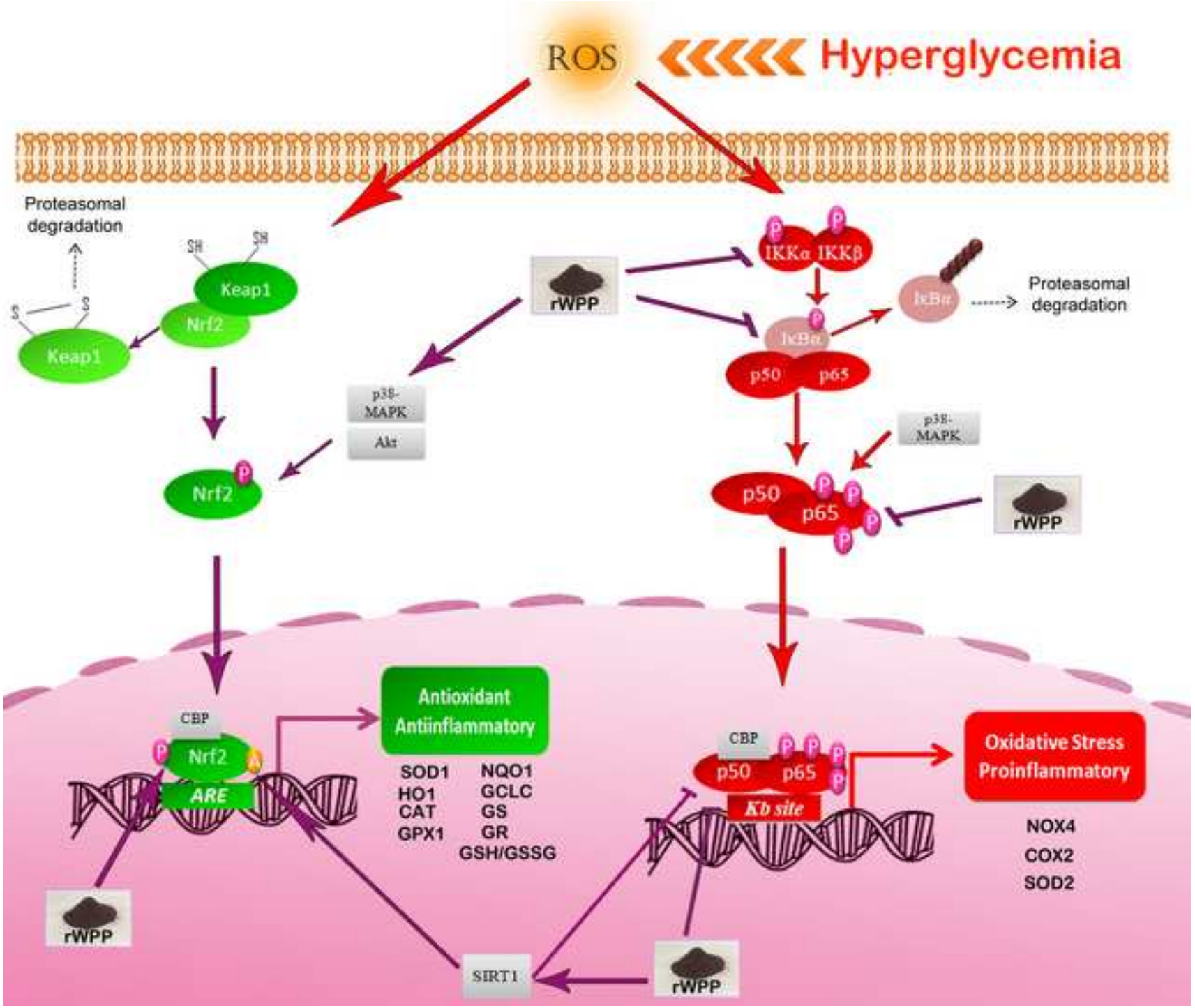

***Conflict of Interest**

Conflicts of interest

Declarations of interest: none

***Ethics Statement**

The research did not include any human subjects and animal experiments.